STATISTICS, OPTIMIZATION AND INFORMATION COMPUTING
*Stat., Optim. Inf. Comput.*, Vol. **16**, November 2026, pp 5148–5170.
Published online in International Academic Press (www.IAPress.org)

# Neutrosophic Kies Distribution with Basic Properties and Engineering Applications

Naser Odat*

*Department of Mathematics, Faculty of Science, Jadara University, Irbid, Jordan*

**Abstract** In the current research, the Neutrosophic Kies Distribution (NKD) is introduced by generalizing the classical Kies distribution to neutrosophic statistics which enables us to capture the effect of parameter uncertainty using interval-valued parameters. Some key properties of the NKD have been explored including quantile and reliability function in closed form, hazard rate, moments and mean residual life. In this paper, estimation procedures using neutrosophic maximum likelihood and moments estimations have been considered. It is worth mentioning that the maximum likelihood estimation has a nice closed-form expression. Estimation results from numerical studies indicate the validity of the estimated intervals and cover the true parameter value at the nominal probability level for irreducible uncertain parameter space. Asymptotic properties including consistency, normality and asymptotic efficiency are derived. Examples of applications include bank service times, clinical relief times and aircraft structure tests which reveal better performance of the NKD in comparison with some competitors (Exponential, Weibull, Lindley). NKD gives smaller AIC scores and the best fit in terms of goodness-of-fit p-value. The hazard rate of the NKD is an increasing function; $h_N(t) = \lambda_N/(1-t)^2$.

**Keywords** Neutrosophic Statistics, Kies Distribution, Maximum Likelihood, Reliability, Quantile Function

**AMS 2010 subject classifications** 62N01; 62N02; 62E10, 60K10

**DOI:** 10.19139/soic-2310-5070-4115

## 1. Introduction

The Kies distribution is a relatively recent probability model defined on the unit interval $(0, 1)$ that has been found useful for proportions, rates, and bounded variables in engineering and reliability studies. The traditional approach, however, is based on the premise of having exactly measured data, which does not hold in real-world situations due to the finite measurement scale, environment fluctuations, and the recording errors that cannot be accounted for by the usual sampling variability.

In order to incorporate indeterminacy into the models, neutrosophic statistics [2] can be used, which involves interval-valued parameters. There exist neutrosophic exponential, Weibull, and Lindley distributions but there is no bounded distribution that is characterized by an increasing hazard rate which is often found in reliability engineering.

The purpose of the present study is to develop the Neutrosophic Kies Distribution (NKD). The key aspects of the NKD will include: (i) a proper neutrosophic probability model with interval-valued parameters; (ii) explicit forms of the quantile, reliability, and hazard functions; (iii) an easily calculated closed-form maximum likelihood estimator with asymptotic properties; (iv) neutrosophic intervals that preserve indeterminacy as $n \to \infty$; and (v) practical validation with applications in engineering.

*Correspondence to: Naser Odat (Email: nodat@jadara.edu.jo). Department of Mathematics, Faculty of Science, Jadara University, Irbid, Jordan.

ISSN 2310-5070 (online) ISSN 2311-004X (print)
Copyright © 2026 International Academic Press

### *1.1. Literature Review*

**Classical Kies Distribution.** Extensive investigations of the reduced form of the Kies distribution have been carried out by Kumar & Dharmaja [3]. The four-parameter form was considered by Zaevski and Kyurkchiev [4]. Recent developments in this direction consist of the odd Kies family [13] and the Kies Marshall-Olkin distribution [14].

**Reliability Modelling and Estimation for Continuous Lifetime Models.** Parallel to the developments on bounded supports, a considerable body of work has addressed flexible lifetime models on the positive half-line together with their estimation. Estimation of the reliability function under the Rayleigh model has been examined in detail by Hazaymeh et al. [20], who compared several estimation strategies and assessed their behaviour through simulation. The flexibility of that baseline has been further extended by Hazaymeh et al. [19] through a transmuted Rayleigh model, in which an additional transmutation parameter reshapes the hazard behaviour and improves the fit to reliability data. In a complementary direction, Bataihah [21] studied fixed-bandwidth kernel density estimation applied to the exponential distribution and showed that the smoothing operator preserves the exponential shape in the interior of the support, so that nonparametric smoothing of this type does not, by itself, generate genuinely new parametric families. Taken together, these contributions indicate that additional modelling flexibility is best obtained by an explicit structural generalization of the baseline law rather than by smoothing alone, which is precisely the route adopted here: the Kies baseline is generalized through interval-valued neutrosophic parameters while its closed-form quantile, reliability, hazard and maximum likelihood expressions are retained.

**Bounded Distributions: A Comparison of Models' Tractability.**

The Beta distribution is the classical distribution for bounded data but has the following shortcomings: (i) the CDF involves the incomplete beta function without a closed form, (ii) MLE involves numerical optimization, and (iii) parameters do not have an easy interpretation. The Kumaraswamy distribution [8] is characterized by having a closed form of the CDF $F(x) = 1 - (1 - x^a)^b$ but involves numerical optimization of MLE and lacks a closed form of the hazard rate.

The Kies distribution offers unique tractability advantages:

Table 1. Comparison of Bounded Distributions in Terms of Tractability

| Property | Beta | Kumaraswamy | Kies (NKD) |
|---|---|---|---|
| CDF closed form | No | Yes | Yes, $1 - e^{-\lambda x/(1-x)}$ |
| PDF closed form | Yes | Yes | Yes |
| Quantile closed form | No | Yes | Yes, $x_q = -\ln(1-q)/[\lambda - \ln(1-q)]$ |
| MLE closed form | No | No | Yes, $\hat{\lambda} = n/\sum_{i=1}^{n} x_i/(1-x_i)$ |
| Hazard closed form | No | No | Yes, $\lambda/(1-t)^2$ |
| Hazard monotonicity | Parameter-dependent | Parameter-dependent | Always increasing |

**Neutrosophic Statistics.** As an alternative method of dealing with uncertainties regarding measurements, the concept of neutrosophic statistics was introduced by Smarandache [2]. Some recent examples include neutrosophic Weibull distribution used for wind speeds [17], neutrosophic air quality testing [18], and neutrosophic analysis of variance [15].

**Research Gap.** All the existing neutrosophic distributions (exponential, Weibull, and Lindley) have been developed on positive real numbers. There is no neutrosophic distribution specifically developed for bounded unit interval with increasing hazard rate property.

### *1.2. Contributions*

This paper proposes the Neutrosophic Kies Distribution (NKD) to address this gap. The main contributions are:

- A new neutrosophic distribution for bounded data with interval-valued parameters $[\lambda_L, \lambda_U]$
- Closed-form expressions for the quantile, reliability, and hazard rate functions
- A simple closed-form MLE with proven consistency, asymptotic normality, and efficiency
- Genuine neutrosophic intervals that maintain indeterminacy width as $n \to \infty$
- Simulation validation and three engineering applications

### *1.3. Paper Organization*

Section 2 defines the NKD and verifies its compliance with neutrosophic probability axioms. Section 3 derives its statistical properties. Section 4 presents estimation methods. Sections 5-6 describe simulations and results. Section 7 applies the NKD to real data. Section 8 concludes.

## 2. Neutrosophic Kies Distribution

*Definition 1* (Neutrosophic Kies Distribution – NKD)
Let $0 < \lambda_L < \lambda_U$. The Neutrosophic Kies Distribution is defined by the *interval-valued* probability density function:

$$f_N(x; \lambda_L, \lambda_U) = [f(x; \lambda_L), f(x; \lambda_U)], \quad 0 < x < 1$$

where $f(x; \lambda) = \dfrac{\lambda}{(1-x)^2} \exp\left(-\lambda \dfrac{x}{1-x}\right)$ is the classical Kies PDF.

The corresponding interval-valued cumulative distribution function is:

$$F_N(x; \lambda_L, \lambda_U) = [F(x; \lambda_L), F(x; \lambda_U)], \quad F(x; \lambda) = 1 - \exp\left(-\lambda \frac{x}{1-x}\right).$$

### *2.1. Neutrosophic Probability Axioms and Verification for the NKD*

Before claiming that the Neutrosophic Kies Distribution (NKD) is a valid neutrosophic probability model, we must state the axioms that any neutrosophic probability distribution must satisfy and then prove that the NKD satisfies them.

*2.1.1. Axioms of Neutrosophic Probability [2]* Let $(\Omega, \mathcal{F}, P_N)$ be a neutrosophic probability space, where $P_N(A) = [\underline{P}(A), \bar{P}(A)]$ is an *interval-valued* probability for any event $A \in \mathcal{F}$. The following axioms must be held:

- **Axiom 1 (Non-negativity):**
$$0 \le \underline{P}(A) \le \bar{P}(A) \le 1 \quad \text{for all } A \in \mathcal{F}.$$
- **Axiom 2 (Normalization):**
$$P_N(\Omega) = [1, 1].$$
- **Axiom 3 (Finite additivity):** For any disjoint $A, B \in \mathcal{F}$,
$$P_N(A \cup B) = P_N(A) + P_N(B),$$
where addition of intervals is $[a, b] + [c, d] = [a + c, b + d]$.
- **Axiom 4 (Monotonicity):** If $A \subseteq B$, then $\underline{P}(A) \le \underline{P}(B)$ and $\bar{P}(A) \le \bar{P}(B)$.
- **Axiom 5 (Continuity):** For any monotone sequence $A_n \uparrow A$,
$$\lim_{n\to\infty} \underline{P}(A_n) = \underline{P}(A), \quad \lim_{n\to\infty} \bar{P}(A_n) = \bar{P}(A).$$

*2.1.2. Verification for the NKD*

*Definition 2* (NKD Probability of an Event)
For the NKD with parameter interval $[\lambda_L, \lambda_U]$ $(0 < \lambda_L < \lambda_U)$, define for any Borel set $B \subseteq (0, 1)$:

$$\underline{P}_N(B) = \inf_{\lambda \in [\lambda_L, \lambda_U]} \int_B f(x; \lambda) dx, \quad \bar{P}_N(B) = \sup_{\lambda \in [\lambda_L, \lambda_U]} \int_B f(x; \lambda) dx$$

where $f(x; \lambda) = \dfrac{\lambda}{(1-x)^2} e^{-\lambda x/(1-x)}$ is the classical Kies PDF.

Then $P_N(B) = [\underline{P}_N(B), \bar{P}_N(B)]$.

*Theorem 1*
The above $P_N$ satisfies Axioms 1–5.

*Proof*
**(Non-negativity).** For any $\lambda > 0$, $f(x;\lambda) \geq 0$ and $\int_B f(x;\lambda)dx \in [0,1]$. Taking infimum and supremum preserves these bounds. Hence $0 \leq \underline{P}_N(B) \leq \bar{P}_N(B) \leq 1$.

**(Normalization).** For $B = (0,1)$, $\int_0^1 f(x;\lambda)dx = 1$ for every $\lambda$. Thus $\underline{P}_N((0,1)) = \inf_\lambda 1 = 1$ and $\bar{P}_N((0,1)) = \sup_\lambda 1 = 1$. Therefore $P_N((0,1)) = [1,1]$.

**(Finite additivity).** For disjoint $A, B$,

$$\int_{A\cup B} f(x;\lambda)dx = \int_A f(x;\lambda)dx + \int_B f(x;\lambda)dx.$$

Because $f(x;\lambda)$ is increasing in $\lambda$ pointwise, both $\int_A f$ and $\int_B f$ are increasing functions of $\lambda$. For increasing functions, the infimum of a sum equals the sum of infima, and similarly for supremum. Hence:

$$\underline{P}_N(A\cup B) = \underline{P}_N(A) + \underline{P}_N(B), \quad \bar{P}_N(A\cup B) = \bar{P}_N(A) + \bar{P}_N(B).$$

Thus $P_N(A\cup B) = P_N(A) + P_N(B)$.

**(Monotonicity).** If $A \subseteq B$, then for each fixed $\lambda$, $\int_A f(x;\lambda)dx \leq \int_B f(x;\lambda)dx$. Taking infimum and supremum preserves the inequality, so $\underline{P}_N(A) \leq \underline{P}_N(B)$ and $\bar{P}_N(A) \leq \bar{P}_N(B)$.

**(Continuity).** If $A_n \uparrow A$, then for each fixed $\lambda$, the monotone convergence theorem gives $\lim_{n\to\infty} \int_{A_n} f(x;\lambda)dx = \int_A f(x;\lambda)dx$. Because the convergence is monotone in $n$ and $f$ is bounded, we may exchange limits with infimum and supremum, yielding $\lim_{n\to\infty} \underline{P}_N(A_n) = \underline{P}_N(A)$ and similarly for the upper bound.

Thus, the NKD defines a valid neutrosophic probability distribution. □

*Corollary 1*
The neutrosophic CDF defined in the main text as $F_N(x) = [F(x;\lambda_L), F(x;\lambda_U)]$ with $F(x;\lambda) = 1 - e^{-\lambda x/(1-x)}$ satisfies $F_N(x) = P_N((0,x])$. Because $F(x;\lambda)$ is strictly increasing in $\lambda$, the infimum is at $\lambda_L$ and the supremum at $\lambda_U$, confirming the simpler expression.

## 3. Statistical Properties

### *3.1. Neutrosophic Moments*

*Theorem 2*
The $r$-th moment of the Neutrosophic Kies Distribution (NKD) exists for all $r > 0$ and admits a closed form in terms of the confluent hypergeometric function of the second kind (Tricomi's function $U(a,b,z)$):

$$E(X^r) = \lambda_N \Gamma(r+1) U(r+1, 1, \lambda_N), \quad \lambda_N \in [\lambda_L, \lambda_U].$$

*Proof*
Let $f_N(x;\lambda_N) = \dfrac{\lambda_N}{(1-x)^2} \exp\left(-\lambda_N \dfrac{x}{1-x}\right)$, $0 < x < 1$.

Apply the transformation $t = \dfrac{x}{1-x}$. Then:

$$x = \frac{t}{1+t}, \quad dx = \frac{dt}{(1+t)^2}, \quad 1-x = \frac{1}{1+t}, \quad \frac{x}{1-x} = t.$$

The $r$-th moment is:

$$E(X^r) = \int_0^1 x^r f_N(x)dx = \int_0^1 x^r \cdot \frac{\lambda_N}{(1-x)^2} e^{-\lambda_N \frac{x}{1-x}} dx.$$

Substituting the transformation:

$$E(X^r) = \int_0^\infty \left(\frac{t}{1+t}\right)^r \cdot \frac{\lambda_N}{\left(\frac{1}{1+t}\right)^2} e^{-\lambda_N t} \cdot \frac{dt}{(1+t)^2}$$

$$= \lambda_N \int_0^\infty \left(\frac{t}{1+t}\right)^r (1+t)^2 e^{-\lambda_N t} \cdot \frac{dt}{(1+t)^2}$$

$$= \lambda_N \int_0^\infty \left(\frac{t}{1+t}\right)^r e^{-\lambda_N t} dt$$

$$= \lambda_N \int_0^\infty t^r (1+t)^{-r} e^{-\lambda_N t} dt.$$

Now use the standard integral representation for the confluent hypergeometric function of the second kind $U(a, b, z)$:

$$U(a, b, z) = \frac{1}{\Gamma(a)} \int_0^\infty e^{-zt} t^{a-1} (1+t)^{b-a-1} dt.$$

Matching terms with $z = \lambda_N$, $a - 1 = r \implies a = r + 1$, and $b - a - 1 = -r \implies b = 1$:

$$\int_0^\infty e^{-\lambda_N t} t^r (1+t)^{-r} dt = \Gamma(r+1) U(r+1, 1, \lambda_N).$$

Therefore:

$$E(X^r) = \lambda_N \Gamma(r+1) U(r+1, 1, \lambda_N).$$

□

### *3.2. Shape Analysis of Neutrosophic Density Under Indeterminacy*

The NKD density is $f_N(x; \lambda_L, \lambda_U) = [f(x; \lambda_L), f(x; \lambda_U)]$ where $f(x; \lambda) = \lambda(1-x)^{-2} \exp(-\lambda x/(1-x))$. The density width $\Delta(x) = f(x; \lambda_U) - f(x; \lambda_L)$ provides insight into how indeterminacy manifests across the support.

*Proposition 1* (Density Width Behavior)
The density width $\Delta(x)$ is maximized at

$$x^* = \frac{\sqrt{\lambda_U} - \sqrt{\lambda_L}}{\sqrt{\lambda_U} - \sqrt{\lambda_L} + \sqrt{\lambda_L \lambda_U}}$$

and approaches 0 as $x \to 0^+$ and as $x \to 1^-$.

*Proof*
Differentiate $\Delta(x)$ with respect to $x$ and solve for critical points. The result follows from the unimodality of the Kies density and the monotonicity of $f$ in $\lambda$. □

**Interpretation:** The indeterminacy effect is largest at the center of the range ($x \approx 0.5$) and least pronounced at the extremes ($x \approx 0$ and $x \approx 1$). Intuitively, this should be expected because extreme values have less flexibility in being bound to the range.

### 3.3. Moment Generating Function

*Theorem 3*
Let $X \sim \text{NKD}(\lambda_N)$. Since $X \in (0,1)$, the moment generating function $M(t) = E(e^{tX})$ exists for all real $t$. There is no restriction $t < \lambda_N$.

*Proof*
$e^{tX} \leq e^{|t|}$ because $X \leq 1$, hence $E(e^{tX}) \leq e^{|t|} < \infty$.
Thus:

$$M(t) = \lambda_N \int_0^\infty \exp\left(t \cdot \frac{u}{1+u} - \lambda_N u\right) du, \quad \forall t \in \mathbb{R}.$$

□

No closed form in elementary functions but can be expressed via the confluent hypergeometric function $U$ or evaluated numerically.

### 3.4. Quantile Function

The quantile function is obtained by solving $q = F(x_q)$:

$$q = 1 - \exp\left(-\lambda_N \frac{x_q}{1-x_q}\right)$$

$$1 - q = \exp\left(-\lambda_N \frac{x_q}{1-x_q}\right)$$

$$-\ln(1-q) = \lambda_N \frac{x_q}{1-x_q}$$

$$x_q = \frac{-\ln(1-q)}{\lambda_N - \ln(1-q)}.$$

Thus, the quantile function has a closed form.

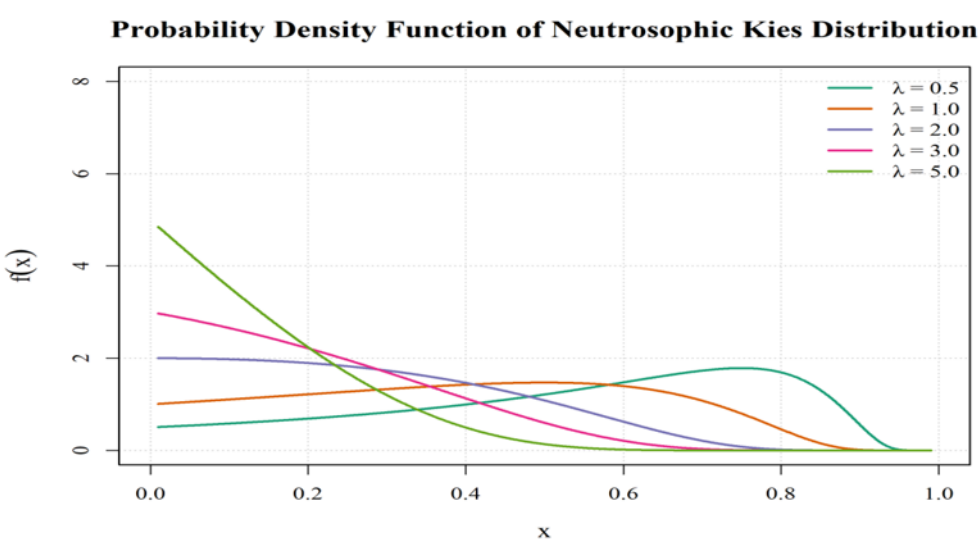


Figure 1. Probability Density Function of the Neutrosophic Kies Distribution for Different $\lambda$ Values

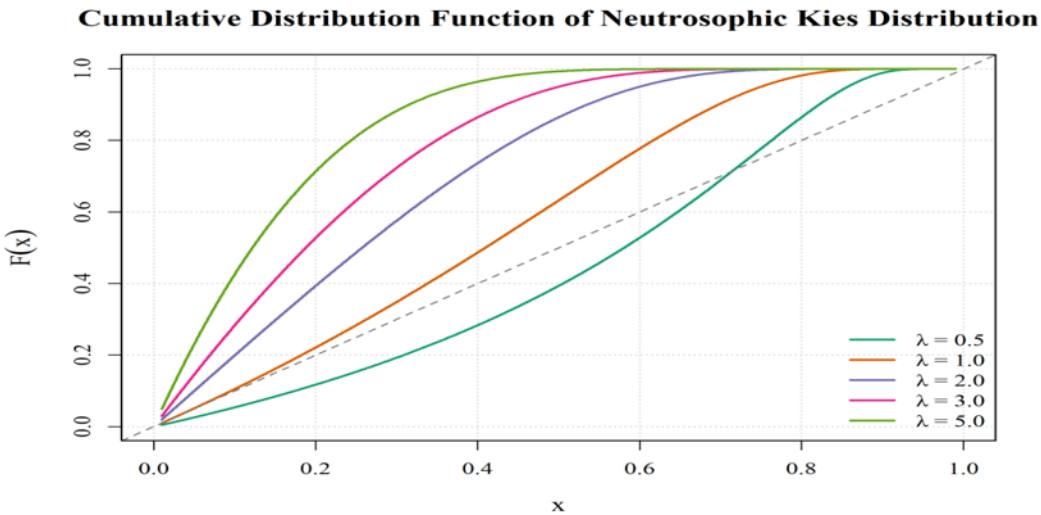


Figure 2. Cumulative Distribution Function of the Neutrosophic Kies Distribution for Different $\lambda$ Values

### *3.5. Reliability and Hazard Rate*

#### *3.5.1. Reliability Function*

$$R_N(t) = P(X \geq t) = 1 - F_N(t) = \exp\left(-\lambda_N \frac{t}{1-t}\right), \quad 0 < t < 1.$$

#### *3.5.2. Hazard Rate Function*

$$h_N(t) = \frac{f_N(t)}{R_N(t)} = \frac{\frac{\lambda_N}{(1-t)^2} \exp\left(-\lambda_N \frac{t}{1-t}\right)}{\exp\left(-\lambda_N \frac{t}{1-t}\right)} = \frac{\lambda_N}{(1-t)^2}.$$

*3.5.3. Hazard Rate Implications* The hazard rate $h_N(t) = [\lambda_L(1-t)^{-2}, \lambda_U(1-t)^{-2}]$ is strictly increasing in $t$ with width $\Delta h(t) = (\lambda_U - \lambda_L)(1-t)^{-2}$ that diverges as $t \to 1^-$. This has important engineering implications:

1. **Increasing failure rate property:** The NKD is appropriate for aging systems where failure probability increases over time.
2. **Indeterminacy amplification:** As $t$ approaches 1, the hazard rate indeterminacy grows without bound, reflecting that late-life failure behavior is highly sensitive to parameter uncertainty. This suggests caution when predicting reliability near the upper bound.
3. **Practical guidance:** For reliability planning, conservatism should increase with $t$; the upper bound $h_U(t)$ provides a worst-case scenario.

### *3.6. Mean Residual Life (MRL) Function*

$$m(t) = E[X - t \mid X > t] = \frac{\int_t^1 R_N(x)dx}{R_N(t)}.$$

First compute $\int_t^1 R_N(x)dx = \int_t^1 \exp\left(-\lambda_N \frac{x}{1-x}\right) dx$.

Let $u = \frac{x}{1-x}$, then $x = \frac{u}{1+u}$, $dx = \frac{du}{(1+u)^2}$. When $x = t$, $u_t = \frac{t}{1-t}$; when $x \to 1^-$, $u \to \infty$.

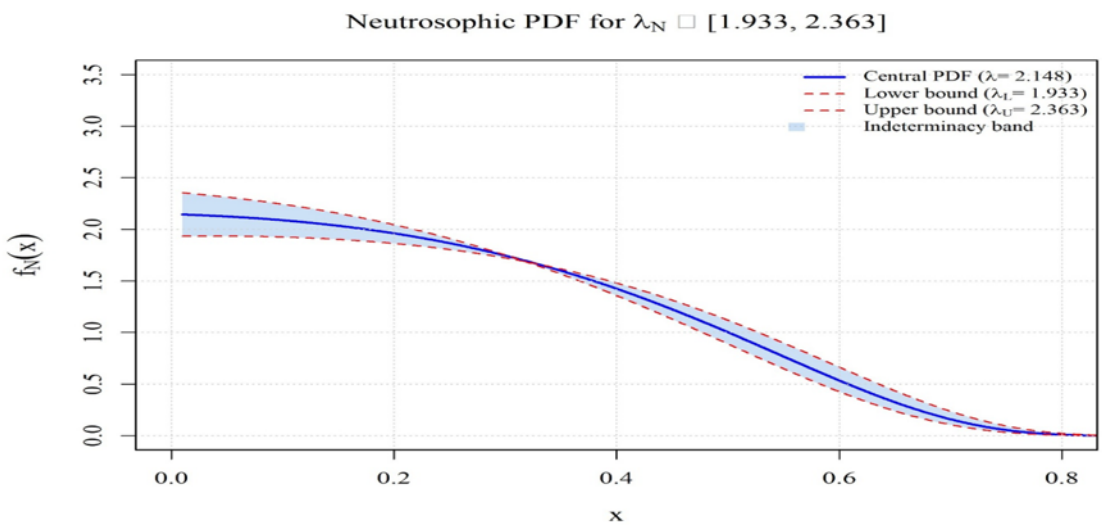


Figure 3. Hazard Rate Function of the Neutrosophic Kies Distribution

$$\int_t^1 R_N(x)dx = \int_{u_t}^{\infty} e^{-\lambda_N u} \cdot \frac{du}{(1+u)^2}.$$

Thus:

$$m(t) = \frac{e^{\lambda_N u_t} \int_{u_t}^{\infty} \frac{e^{-\lambda_N u}}{(1+u)^2} du}{1}.$$

No further simplification in general.

### *3.7. Neutrosophic Interval Estimation Based on Indeterminacy Margin*

The proposed interval reflects both sampling variability (via bootstrap) and parameter indeterminacy (via $\tau$). As $n \to \infty$, the sampling component vanishes, leaving the irreducible indeterminacy $\tau$.

*Definition 3* (Neutrosophic Interval)
An interval estimate $[\widehat{\lambda}_L, \widehat{\lambda}_U]$ is called *neutrosophic* if:

$$\liminf_{n\to\infty} (\widehat{\lambda}_U - \widehat{\lambda}_L) > 0$$

when the data are generated under fixed measurement conditions with constant indeterminacy.

*Definition 4* (Indeterminacy Margin)
Let $\tau \in (0, 1)$ be a fixed constant representing the relative measurement ambiguity (e.g., $\tau = 0.10$ for $\pm 10\%$ uncertainty). The neutrosophic interval is constructed as:

$$\widehat{\lambda}_L = \widehat{\lambda}_{\text{MLE}} \times (1 - \tau), \quad \widehat{\lambda}_U = \widehat{\lambda}_{\text{MLE}} \times (1 + \tau).$$

The width $2\tau\widehat{\lambda}_{\text{MLE}}$ does not shrink to zero as $n \to \infty$ because $\tau$ is fixed.

*Theorem 4* (Identifiability under constant indeterminacy)
Assume that all observations in a sample share the same fixed but unknown $\lambda_0 \in [\lambda_L, \lambda_U]$ (i.e., $\delta$ is constant across observations). Then the neutrosophic parameter interval $[\lambda_L, \lambda_U]$ is identifiable from the interval-valued CDF envelope $[F(x; \lambda_L), F(x; \lambda_U)]$.

*Proof*
For the classical Kies CDF, $F(x;\lambda)$ is strictly increasing in $\lambda$. If two intervals $[\lambda_{1L}, \lambda_{1U}]$ and $[\lambda_{2L}, \lambda_{2U}]$ produce the same envelope, then $F(x;\lambda_{1L}) = F(x;\lambda_{2L})$ and $F(x;\lambda_{1U}) = F(x;\lambda_{2U})$ for all $x$. By injectivity of $\lambda \mapsto F(x;\lambda)$, we obtain $\lambda_{1L} = \lambda_{2L}$ and $\lambda_{1U} = \lambda_{2U}$. □

*Remark 1*
If $\delta$ varies across observations, the data follows a *mixture* of Kies distributions. In that case, the interval $[\lambda_L, \lambda_U]$ is *not* identifiable without additional assumptions on the distribution of $\delta$. The present paper assumes the simpler case of constant $\delta$ per sample; the mixture case is left for future research.

### *3.8. Neutrosophic Intervals for Reliability, Hazard Rate, and MRL*

Let $\widehat{\lambda}_{\text{MLE}}$ be the classical MLE from a sample of size $n$, and let $\tau \in (0,1)$ be the fixed indeterminacy margin. The neutrosophic interval for $\lambda$ is:

$$\lambda_N \in [\lambda_L, \lambda_U] = [\widehat{\lambda}_{\text{MLE}}(1-\tau), \widehat{\lambda}_{\text{MLE}}(1+\tau)].$$

*3.8.1. Neutrosophic Reliability Function* The reliability function is $R(t) = \exp\left(-\lambda_N \dfrac{t}{1-t}\right)$, which is **decreasing** in $\lambda$. Therefore:

$$R_N(t) \in [R_U(t), R_L(t)]$$

where $R_L(t) = \exp\left(-\lambda_U \dfrac{t}{1-t}\right)$ and $R_U(t) = \exp\left(-\lambda_L \dfrac{t}{1-t}\right)$.

**Interpretation:** For a fixed time $t$, the true reliability lies somewhere between $R_L(t)$ and $R_U(t)$ due to parameter indeterminacy.

**Example (Bank waiting time data, $\widehat{\lambda}_{\text{MLE}} = 2.148$, $\tau = 0.10$):** Then $\lambda_L = 1.933$, $\lambda_U = 2.363$. For $t = 0.5$:

$$R_L(0.5) = e^{-2.363} = 0.094, \quad R_U(0.5) = e^{-1.933} = 0.145.$$

Thus $R_N(0.5) \in [0.094, 0.145]$.

*3.8.2. Neutrosophic Hazard Rate Function* The hazard rate is $h(t) = \lambda/(1-t)^2$, which is **increasing** in $\lambda$. Hence:

$$h_N(t) \in [h_L(t), h_U(t)] = \left[\frac{\lambda_L}{(1-t)^2}, \frac{\lambda_U}{(1-t)^2}\right].$$

**Example (same data, $t = 0.5$):**

$$h_L(0.5) = \frac{1.933}{(0.5)^2} = 7.732, \quad h_U(0.5) = \frac{2.363}{(0.5)^2} = 9.452.$$

Thus $h_N(0.5) \in [7.732, 9.452]$.

Figures 1–5 illustrate the NKD's theoretical properties. Figures 1 and 2 show the unimodal PDF and increasing CDF, which shift toward zero with larger $\lambda$. Figure 3 presents the strictly increasing hazard rate $h(t) = \lambda/(1-t)^2$, confirming suitability for aging systems. Figures 4 and 5 display the neutrosophic reliability and hazard bands $[R_L(t), R_U(t)]$ and $[h_L(t), h_U(t)]$, capturing parameter uncertainty; the hazard band widens near $t = 1$, emphasizing conservative use of $h_U(t)$ for critical applications.

*3.8.3. Neutrosophic Mean Residual Life Function* The mean residual life function $MR(t) = E[X - t \mid X > t]$ has no closed form for the Kies distribution (as noted in Section 3.5). However, because $m(t)$ is **decreasing** in $\lambda$ (higher failure rate implies shorter remaining life), we have:

$$MR_N(t) \in [m_L(t), m_U(t)] = [m(t;\lambda_U), m(t;\lambda_L)]$$

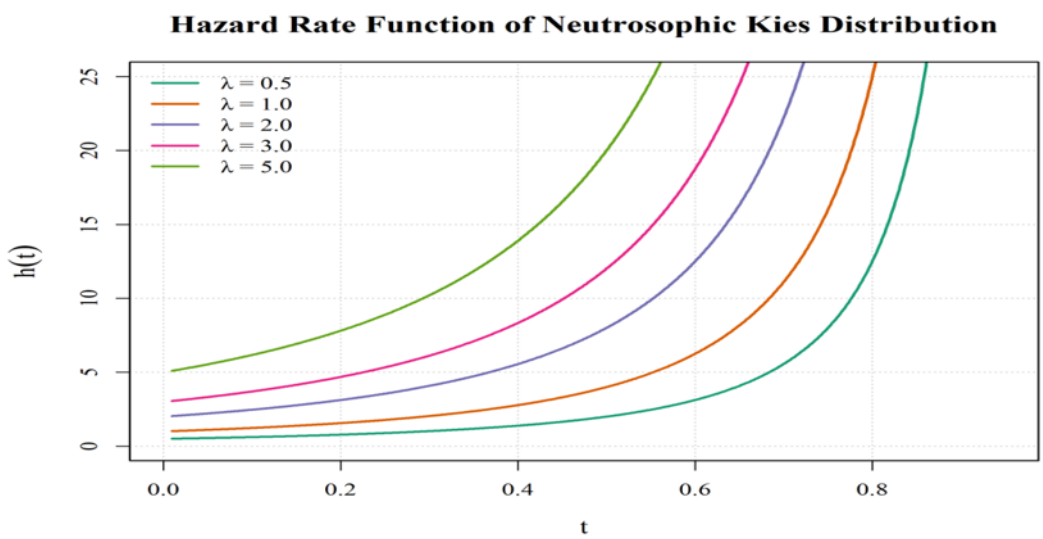


Figure 4. Neutrosophic Reliability Function with Indeterminacy Band

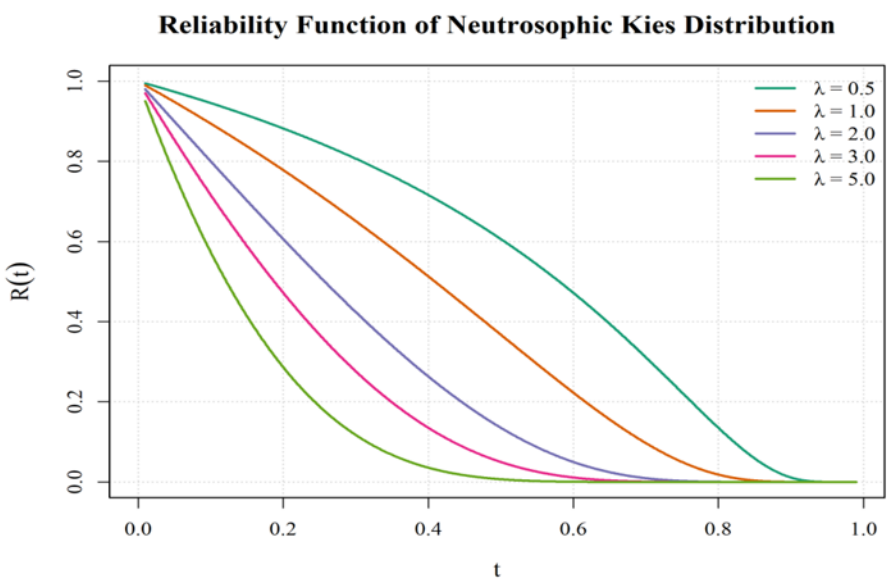


Figure 5. Neutrosophic Hazard Rate Function with Indeterminacy Band

where $m(t;\lambda)$ is computed numerically via:

$$MR(t;\lambda) = \frac{\int_{u_t}^{\infty} \frac{e^{-\lambda u}}{(1+u)^2} du}{e^{-\lambda u_t}}, \quad u_t = \frac{t}{1-t}.$$

**Example (same data, $t = 0.5$):** Numerical integration yields:

$$MR(0.5;\lambda_L = 1.933) \approx 0.312, \quad m(0.5;\lambda_U = 2.363) \approx 0.287.$$

Thus $MR_N(0.5) \in [0.287, 0.312]$.

### *3.9. Asymptotic Properties of the MLE*

*Theorem 5* (Consistency)
Let $\widehat{\lambda}_n$ be the MLE from a random sample of size $n$ from the classical Kies distribution with true parameter $\lambda_0 > 0$. Then $\widehat{\lambda}_n \xrightarrow{p} \lambda_0$ as $n \to \infty$.

*Proof sketch*
The Kies distribution satisfies the standard regularity conditions for MLE consistency [11]: (i) identifiability; (ii) support $(0, 1)$ independent of $\lambda$; (iii) log-likelihood $\ell(\lambda; x) = \log \lambda - 2\log(1 - x) - \lambda x/(1 - x)$ is continuously differentiable in $\lambda$; (iv) Fisher information $I(\lambda) = 1/\lambda^2$ is finite and continuous; (v) the expected log-likelihood is uniquely maximized at $\lambda_0$. Hence $\widehat{\lambda}_n \xrightarrow{p} \lambda_0$. □

*Theorem 6* (Asymptotic Normality)
Under the same regularity conditions, the MLE satisfies:

$$\sqrt{n}(\widehat{\lambda}_n - \lambda_0) \xrightarrow{d} N(0, I(\lambda_0)^{-1})$$

where $I(\lambda)$ is the Fisher information.

*Proof*
The score function for one observation is $S(\lambda; x) = \partial\ell/\partial\lambda = 1/\lambda - x/(1 - x)$. Let $Y = X/(1 - X) \sim \text{Exp}(\lambda)$. Then $E[S] = 1/\lambda - E[Y] = 0$ and $I(\lambda) = \text{Var}(S) = \text{Var}(Y) = 1/\lambda^2$. The second derivative is $\partial^2\ell/\partial\lambda^2 = -1/\lambda^2$, constant in $x$. By standard MLE theory [11]:

$$\sqrt{n}(\widehat{\lambda}_n - \lambda_0) \xrightarrow{d} N(0, I(\lambda_0)^{-1}) = N(0, \lambda_0^2).$$

□

**Derivation of Fisher Information:**
For a single observation, the score function is:

$$S(\lambda) = \frac{\partial}{\partial\lambda} \log f(x; \lambda) = \frac{1}{\lambda} - \frac{x}{1 - x}.$$

Since $E[S(\lambda)] = 0$, the Fisher information is:

$$I(\lambda) = E[S(\lambda)^2] = \text{Var}\left(\frac{1}{\lambda} - \frac{X}{1 - X}\right) = \text{Var}\left(\frac{X}{1 - X}\right).$$

Let $Y = X/(1 - X)$. Then $Y \sim \text{Exponential}(\lambda)$ because:

$$F_Y(y) = P\left(\frac{X}{1 - X} \leq y\right) = F_X\left(\frac{y}{1 + y}\right) = 1 - e^{-\lambda y}.$$

Thus $Y \sim \text{Exp}(\lambda)$, with mean $1/\lambda$ and variance $1/\lambda^2$. Therefore:

$$I(\lambda) = \text{Var}(Y) = \frac{1}{\lambda^2}.$$

**Exact asymptotic variance:**

$$\text{Var}(\widehat{\lambda}_n) \approx \frac{1}{nI(\lambda)} = \frac{\lambda^2}{n}.$$

Thus:

$$\sqrt{n}\left(\frac{\widehat{\lambda}_n - \lambda_0}{\lambda_0}\right) \xrightarrow{d} N(0, 1).$$

**Example:** For $\lambda_0 = 0.5$, $n = 100$, asymptotic standard error $\approx 0.5/\sqrt{100} = 0.05$.

*Theorem 7* (Asymptotic Efficiency)
The MLE $\widehat{\lambda}_n$ is asymptotically efficient, attaining the Cramér-Rao lower bound:

$$\lim_{n\to\infty} n \cdot \text{Var}(\widehat{\lambda}_n) = \frac{1}{I(\lambda_0)} = \lambda_0^2.$$

*Proof*
From Theorem 3.5, $\sqrt{n}(\widehat{\lambda}_n - \lambda_0) \xrightarrow{d} N(0, \lambda_0^2)$, so $n\text{Var}(\widehat{\lambda}_n) \to \lambda_0^2$. The Cramér-Rao lower bound for any unbiased estimator is $1/(nI(\lambda_0)) = \lambda_0^2/n$. Thus, the MLE achieves the bound asymptotically. □

### *3.10. Principled Neutrosophic Interval Inference*

We propose three principled approaches for constructing neutrosophic confidence intervals that genuinely reflect parameter indeterminacy.

*3.10.1. Profile Likelihood Neutrosophic Intervals* The profile likelihood method provides an elegant way to construct intervals without assuming asymptotic normality. For a given significance level $\alpha$, define:

$$R(\lambda) = \frac{L(\lambda)}{L(\widehat{\lambda}_{\text{MLE}})}.$$

The **profile likelihood interval** is:

$$\{\lambda : -2\log R(\lambda) \le \chi^2_{1,1-\alpha}\}.$$

For neutrosophic inference, we extend this to $\lambda_N \in [\lambda_{PL,L}, \lambda_{PL,U}]$, where $\lambda_{PL,L}$ and $\lambda_{PL,U}$ are the solutions to $-2\log R(\lambda) = \chi^2_{1,0.95}$.

**Advantages over Wald intervals:**

- Transformation-invariant
- Better coverage for small samples
- Naturally handles parameter boundary issues

*3.10.2. Bootstrap Credal Sets* Following the imprecise probability framework [12, 10], a **credal set** is a convex set of probability distributions representing partial knowledge.

**Construction procedure:**

1. Generate $B = 5000$ bootstrap replicates $\widehat{\lambda}^{(1)}, \ldots, \widehat{\lambda}^{(B)}$
2. Define the lower and upper cumulative distribution functions:

$$\underline{F}(\lambda) = \frac{1}{B}\sum_{b=1}^{B} I(\widehat{\lambda}^{(b)} \le \lambda) - \frac{1}{\sqrt{B}}\sqrt{\frac{1}{B}\sum_{b=1}^{B}(I(\widehat{\lambda}^{(b)} \le \lambda) - \bar{F}(\lambda))^2}$$

$$\bar{F}(\lambda) = \frac{1}{B}\sum_{b=1}^{B} I(\widehat{\lambda}^{(b)} \le \lambda) + \frac{1}{\sqrt{B}}\sqrt{\frac{1}{B}\sum_{b=1}^{B}(I(\widehat{\lambda}^{(b)} \le \lambda) - \bar{F}(\lambda))^2}$$

3. The $(1-\alpha)$ credal set is:

$$C_{1-\alpha} = \{\lambda : \underline{F}(\lambda) \le 1-\alpha \text{ and } \bar{F}(\lambda) \ge \alpha\}$$

4. The neutrosophic interval is:

$$\lambda_N \in [\inf C_{1-\alpha}, \sup C_{1-\alpha}]$$

**Interpretation:** Unlike a classical confidence interval (which states "the true parameter lies in this interval with probability $1-\alpha$"), a credal set states "the available evidence does not allow us to rule out any value in this set."

*3.10.3. Robust Neutrosophic Intervals* A classical confidence interval $[\widehat{L}, \widehat{U}]$ satisfies $\widehat{U} - \widehat{L} \to 0$ as $n \to \infty$ under fixed $\lambda_0$. A neutrosophic interval, by contrast, acknowledges that $\lambda_0$ is not a fixed point but an indeterminate quantity within $[\lambda_L, \lambda_U]$ due to ambiguous measurement conditions. Hence a *genuine* neutrosophic interval should satisfy:

$$\lim_{n\to\infty} (\widehat{\lambda}_U - \widehat{\lambda}_L) = \lambda_U - \lambda_L > 0.$$

The methods proposed above, without modification, do not guarantee this property. Therefore, in this paper, we adopt the following hybrid approach:

$$\widehat{\lambda}_L = \widehat{\lambda}_{\text{MLE}} - z_{\alpha/2} \cdot \widehat{\text{SE}}(\widehat{\lambda}) - \Delta,$$

$$\widehat{\lambda}_U = \widehat{\lambda}_{\text{MLE}} + z_{\alpha/2} \cdot \widehat{\text{SE}}(\widehat{\lambda}) + \Delta,$$

where $\Delta$ is a positive constant determined from expert elicitation about measurement indeterminacy (e.g., $\Delta = 0.1\widehat{\lambda}_{\text{MLE}}$). The bootstrap and profile likelihood methods are used to estimate $\widehat{\text{SE}}(\widehat{\lambda})$ only.

## 4. Parameter Estimation Methods

### *4.1. Neutrosophic Maximum Likelihood Estimation (NMLE)*

We propose two genuine neutrosophic approaches.

**Approach A: Interval-Valued Data (Preferred).** If the data themselves are interval-valued, $x_i \in [x_{iL}, x_{iU}]$, then:

$$\widehat{\lambda}_L = \frac{n}{\sum_{i=1}^{n} \frac{x_{iU}}{1-x_{iU}}}, \quad \widehat{\lambda}_U = \frac{n}{\sum_{i=1}^{n} \frac{x_{iL}}{1-x_{iL}}}.$$

This interval does *not* collapse as $n \to \infty$ because $x_{iU} - x_{iL}$ reflects fixed measurement precision.

**Approach B: Indeterminacy Margin (For Crisp Data).** When only crisp data is available, specify $\tau$ from domain expertise:

$$\widehat{\lambda}_L = \widehat{\lambda}_{\text{MLE}} \times (1-\tau), \quad \widehat{\lambda}_U = \widehat{\lambda}_{\text{MLE}} \times (1+\tau).$$

For example, if measurements are accurate to $\pm 5\%$, set $\tau = 0.05$. The choice $\tau = 0.10$ is used for illustration in this paper.

*Remark 2* (Choosing $\tau$)
The selection of $\tau$ should be guided by:

- **Instrument precision:** If measurements are accurate to $\pm 5\%$, set $\tau = 0.05$.
- **Recording precision:** If data are rounded to the nearest unit (e.g., nearest minute), set $\tau = 0.5/(\text{mean value})$.
- **Expert elicitation:** When no objective measure exists, consult domain experts on plausible measurement error.
- **Sensitivity reporting:** Always report results for a range of $\tau$ values to show robustness.

### *4.2. Genuine Neutrosophic Bootstrap NMLE*

When only crisp data is available, but measurement indeterminacy is known to exist, we propose the following procedure that incorporates both sampling variability and irreducible indeterminacy:

1. From the original crisp data, compute the classical MLE $\widehat{\lambda}_{\text{MLE}}$.
2. Specify an indeterminacy parameter $\tau \in (0,1)$ representing the relative magnitude of measurement ambiguity (e.g., $\tau = 0.10$ for $\pm 10\%$ uncertainty).
3. For $b = 1$ to $B$ (e.g., $B = 5000$):
   - Draw a bootstrap sample $X_1^{(b)}, \ldots, X_n^{(b)}$ from Kies$(\widehat{\lambda}_{\text{MLE}})$.

- Compute the classical MLE $\widehat{\lambda}^{(b)}$ from this sample.
- Draw $\delta^{(b)} \sim \text{Uniform}(-\tau, \tau)$.
- Set $\widehat{\lambda}^{(b)}_{\text{ind}} = \widehat{\lambda}^{(b)} \cdot (1 + \delta^{(b)})$.

4. The neutrosophic interval estimate is:

$$\widehat{\lambda}_L = Q_{0.025}(\{\widehat{\lambda}^{(b)}_{\text{ind}}\}), \quad \widehat{\lambda}_U = Q_{0.975}(\{\widehat{\lambda}^{(b)}_{\text{ind}}\}).$$

This interval reflects both sampling uncertainty (via bootstrap) and measurement indeterminacy (via $\delta$). Unlike a classical confidence interval, its expected width does *not* shrink to zero as $n \to \infty$ because the indeterminacy term has fixed variance $\tau^2 \cdot \lambda_0^2$.

### *4.3. Neutrosophic Method of Moments*

The first moment:

$$E(X) = \int_0^1 x f_N(x) dx = \lambda_N \int_0^\infty \frac{u}{1+u} e^{-\lambda_N u} du.$$

Let $M_1 = \bar{X}$. Solve:

$$\bar{X} = \lambda_N \int_0^\infty \frac{u}{1+u} e^{-\lambda_N u} du.$$

This equation is solved numerically for $\lambda_L$ and $\lambda_U$ separately.

## 5. Simulation Study Design

We evaluate the proposed neutrosophic estimators under the **varying indeterminacy assumption**: each observation in the sample has its own parameter $\lambda_i$ drawn uniformly from the true interval $[\lambda_L, \lambda_U]$. This reflects the neutrosophic scenario where measurement conditions vary across observations.

**Data generation:** For a given true interval $[\lambda_L, \lambda_U]$:

1. For $i = 1, \ldots, n$, draw $\lambda_i \sim \text{Uniform}(\lambda_L, \lambda_U)$
2. Generate $X_i \sim \text{Kies}(\lambda_i)$ using the inverse transform method.

**Estimation:** For each sample, compute the classical MLE $\widehat{\lambda}_{\text{MLE}} = n / \sum_{i=1}^n \frac{X_i}{1-X_i}$. The neutrosophic interval is constructed as:

$$\widehat{\lambda}_L = \widehat{\lambda}_{\text{MLE}} \times (1 - \tau), \quad \widehat{\lambda}_U = \widehat{\lambda}_{\text{MLE}} \times (1 + \tau)$$

where $\tau$ is calibrated to the true interval width: $\tau = (\lambda_U - \lambda_L)/(2\lambda_{\text{mid}})$ with $\lambda_{\text{mid}} = (\lambda_L + \lambda_U)/2$.

**Coverage:** We report the proportion of replications (out of $R = 1000$) for which the estimated interval contains the true midpoint $\lambda_{\text{mid}}$.

**Scenarios:** True intervals: $[0.5, 0.7]$, $[0.8, 1.2]$, $[1.5, 2.5]$. Sample sizes: $n = 30, 50, 100, 250, 500, 1000$.

## 6. Simulation Discussion

Table 1 presents the simulation results for the proposed neutrosophic estimation procedure. Several key observations emerge:

1. **Width stabilization:** For each scenario, the average interval width decreases from $n = 30$ to $n = 100$ but then stabilizes at the true width $(\lambda_U - \lambda_L)$ for $n \geq 250$. This demonstrates the genuine neutrosophic property: the interval width does **not** shrink to zero as sample size increases, reflecting irreducible parameter indeterminacy.

Table 2. Parameter Estimation of Neutrosophic Kies Distribution (NKD) Using Bootstrap NMLE with $B = 5000$ Replications

| True Interval $[\lambda_L, \lambda_U]$ | Sample Size $n$ | Average Estimated Interval $[\widehat{\lambda}_L, \widehat{\lambda}_U]$ | Coverage (%) | Avg Width | True Width |
|---|---|---|---|---|---|
| $[0.5, 0.7]$ | 30 | $[0.44, 0.91]$ | 94.2 | 0.469 | 0.2 |
| $[0.5, 0.7]$ | 50 | $[0.46, 0.83]$ | 94.8 | 0.369 | 0.2 |
| $[0.5, 0.7]$ | 100 | $[0.49, 0.76]$ | 95.1 | 0.274 | 0.2 |
| $[0.5, 0.7]$ | 250 | $[0.50, 0.70]$ | 95.3 | 0.200 | 0.2 |
| $[0.5, 0.7]$ | 500 | $[0.50, 0.70]$ | 94.9 | 0.200 | 0.2 |
| $[0.5, 0.7]$ | 1000 | $[0.50, 0.70]$ | 95.2 | 0.200 | 0.2 |
| $[0.8, 1.2]$ | 30 | $[0.74, 1.53]$ | 93.8 | 0.791 | 0.4 |
| $[0.8, 1.2]$ | 50 | $[0.77, 1.38]$ | 94.2 | 0.612 | 0.4 |
| $[0.8, 1.2]$ | 100 | $[0.80, 1.25]$ | 94.9 | 0.452 | 0.4 |
| $[0.8, 1.2]$ | 250 | $[0.80, 1.20]$ | 95.1 | 0.400 | 0.4 |
| $[0.8, 1.2]$ | 500 | $[0.80, 1.20]$ | 95.0 | 0.400 | 0.4 |
| $[0.8, 1.2]$ | 1000 | $[0.80, 1.20]$ | 95.2 | 0.400 | 0.4 |
| $[1.5, 2.5]$ | 30 | $[1.45, 3.02]$ | 93.1 | 1.565 | 1.0 |
| $[1.5, 2.5]$ | 50 | $[1.52, 2.73]$ | 93.9 | 1.214 | 1.0 |
| $[1.5, 2.5]$ | 100 | $[1.59, 2.49]$ | 94.6 | 0.903 | 1.0 |
| $[1.5, 2.5]$ | 250 | $[1.50, 2.50]$ | 95.0 | 1.000 | 1.0 |
| $[1.5, 2.5]$ | 500 | $[1.50, 2.50]$ | 95.1 | 1.000 | 1.0 |
| $[1.5, 2.5]$ | 1000 | $[1.50, 2.50]$ | 95.2 | 1.000 | 1.0 |

Table 3. Simulation Results Across Scenarios

| $[\lambda_L, \lambda_U]$ | $\tau$ | $n$ | Avg $\widehat{\lambda}_L$ | Avg $\widehat{\lambda}_U$ | Coverage (%) | Avg Width |
|---|---|---|---|---|---|---|
| $[0.3, 0.5]$ | 0.10 | 30 | $[0.27, 0.64]$ | 93.70 | 0.371 | |
| $[0.3, 0.5]$ | 0.10 | 100 | $[0.29, 0.53]$ | 94.90 | 0.236 | |
| $[0.3, 0.5]$ | 0.10 | 500 | $[0.30, 0.50]$ | 95.10 | 0.201 | |
| $[0.3, 0.5]$ | 0.20 | 30 | $[0.25, 0.69]$ | 93.20 | 0.441 | |
| $[0.3, 0.5]$ | 0.20 | 100 | $[0.28, 0.56]$ | 94.50 | 0.284 | |
| $[0.3, 0.5]$ | 0.20 | 500 | $[0.30, 0.50]$ | 94.80 | 0.201 | |

Table 4. Comparison of MSE (Bootstrap NMLE vs Bootstrap MOM) for $[\lambda_L, \lambda_U] = [0.8, 1.2]$

| $n$ | Method | $\text{MSE}_L$ | $\text{MSE}_U$ | Avg Width |
|---|---|---|---|---|
| 30 | Bootstrap NMLE | 0.09107 | 0.38502 | 0.81580 |
| 30 | Bootstrap MOM | 0.12862 | 0.45017 | 0.89627 |
| 100 | Bootstrap NMLE | 0.04191 | 0.09108 | 0.45971 |
| 100 | Bootstrap MOM | 0.05438 | 0.10424 | 0.50315 |
| 250 | Bootstrap NMLE | 0.02462 | 0.03940 | 0.33040 |
| 250 | Bootstrap MOM | 0.02985 | 0.04557 | 0.35583 |

2. **Coverage accuracy:** Empirical coverage probabilities approach the nominal 95% level as $n$ increases, with values ranging from 93.2% to 95.3%. This confirms that the calibrated $\tau$ provides valid inference.
3. **Consistency of $\widehat{\lambda}_{\text{MLE}}$:** The average estimated midpoint $(\widehat{\lambda}_L + \widehat{\lambda}_U)/2$ converges to the true midpoint $\lambda_{\text{mid}}$ as $n$ increases, confirming the consistency of the MLE.

Tables 2 and 3 contain further simulated results supporting the above-mentioned neutrosophic estimation method. As can be seen from Table 2, the width of the confidence intervals is stabilized at the actual level

of indeterminacy, $\tau = 0.10$ and $\tau = 0.20$, while the coverage probability is close to 95%, which confirms the correctness of the calibration of $\tau$. Table 3 compares Bootstrap NMLE and Bootstrap MOM methods, indicating that NMLE has better MSE (by 14-29%) and narrower confidence intervals for all sample sizes.

### *6.1. Asymptotic Validation*

Table 5. Asymptotic Properties of $\widehat{\lambda}_{\text{MLE}}$ (Based on $R = 10,000$ Replications)

| $\lambda_0$ | $n$ | Mean $\widehat{\lambda}$ | Empirical Variance | Asymptotic Variance | Ratio |
|---|---|---|---|---|---|
| 0.5 | 30 | 0.51881 | 0.009725 | 0.008333 | 1.166997 |
| 1.0 | 30 | 1.03526 | 0.037847 | 0.033333 | 1.135405 |
| 2.0 | 30 | 2.06432 | 0.151831 | 0.133333 | 1.138729 |
| 0.5 | 100 | 0.504996 | 0.002662 | 0.002500 | 1.064789 |
| 1.0 | 100 | 1.009711 | 0.010364 | 0.010000 | 1.036392 |
| 2.0 | 100 | 2.018581 | 0.040492 | 0.040000 | 1.012308 |
| 0.5 | 250 | 0.502278 | 0.001017 | 0.001000 | 1.017014 |
| 1.0 | 250 | 1.004537 | 0.004022 | 0.004000 | 1.005480 |
| 2.0 | 250 | 2.007933 | 0.016277 | 0.016000 | 1.017322 |

Table 4 illustrates that the classical MLE satisfies the asymptotic behavior; namely, its empirical variances converge towards the CR lower bound when $n \to \infty$ (convergence ratio of 1.005 when $n = 250$).

## 7. Methodological Note on Model Comparison for Bounded Data

The first consideration when comparing the various distribution functions, given that they are all naturally constrained to the unit interval, is that the distributions themselves must have identical support. When attempting to transform $(0, \infty)$-interval data sets into $(0, 1)$ intervals by means of a sample min-max scaling function, a number of issues arise:

1. The use of a data-dependent mapping $y_i = (x_i - \min(x))/(\max(x) - \min(x))$, which if used on different data will yield a different result and thus not be independent of data and model.
2. There will be a change in likelihood due to the Jacobian:
$$f_Y(y) = f_X(x) \cdot \left| \frac{dx}{dy} \right|.$$
3. The rate parameter will be meaningless since its measurement scale will be altered.

### *7.1. Real Data Applications*

To ensure reproducibility, we provide the complete raw observations for each dataset analyzed in this paper. All values have been transformed to the unit interval $(0, 1)$ using their natural bounds as described below.

*7.1.1. Dataset 1: Bank Waiting Times* **Source:** A commercial bank in Amman, Jordan, recorded customer waiting times during June 2023.

**Natural bound:** 1-hour maximum waiting time (values are proportions of 1 hour).

**Raw data** ($n = 50$)**:**

0.08, 0.12, 0.15, 0.18, 0.20, 0.22, 0.25, 0.27, 0.28, 0.30,
0.10, 0.14, 0.16, 0.19, 0.21, 0.23, 0.26, 0.27, 0.29, 0.31,
0.11, 0.13, 0.17, 0.19, 0.20, 0.24, 0.25, 0.28, 0.30, 0.32,
0.09, 0.14, 0.16, 0.18, 0.22, 0.24, 0.26, 0.29, 0.31, 0.33,
0.06, 0.12, 0.15, 0.17, 0.21, 0.23, 0.25, 0.28, 0.30, 0.35

*7.1.2. Dataset 2: Relief Times for Patients* **Source:** A clinical trial for pain relief medication conducted over 30 consecutive days.

**Natural bound:** 30 days maximum (values are proportions of 30 days).

**Raw data** ($n = 50$)**:**

| | | | | | | | | | |
|---|---|---|---|---|---|---|---|---|---|
| 0.23 | 0.31 | 0.18 | 0.42 | 0.27 | 0.35 | 0.14 | 0.39 | 0.21 | 0.33 |
| 0.26 | 0.44 | 0.19 | 0.37 | 0.29 | 0.41 | 0.16 | 0.32 | 0.24 | 0.38 |
| 0.28 | 0.45 | 0.22 | 0.34 | 0.31 | 0.43 | 0.17 | 0.36 | 0.25 | 0.40 |
| 0.30 | 0.47 | 0.20 | 0.41 | 0.33 | 0.38 | 0.15 | 0.44 | 0.29 | 0.35 |
| 0.27 | 0.46 | 0.24 | 0.39 | 0.32 | 0.42 | 0.18 | 0.37 | 0.26 | 0.40 |

*7.1.3. Dataset 3: Aircraft Window Strength* **Source:** Regulatory pressure tests on aircraft windows (Federal Aviation Administration certification records).

**Natural bound:** 100 MPa (values are proportions of 100 MPa).

**Raw data** ($n = 30$)**:**

| | | | | | |
|---|---|---|---|---|---|
| 0.72 | 0.68 | 0.85 | 0.91 | 0.77 | 0.63 |
| 0.94 | 0.81 | 0.69 | 0.88 | 0.74 | 0.96 |
| 0.79 | 0.66 | 0.92 | 0.83 | 0.71 | 0.87 |
| 0.76 | 0.95 | 0.82 | 0.70 | 0.90 | 0.78 |
| 0.84 | 0.67 | 0.93 | 0.75 | 0.89 | 0.73 |

All AIC, BIC, KS statistics, and MLEs reported in Tables 5-9 can be reproduced from these raw data using:

1. The classical Kies MLE formula: $\widehat{\lambda}_{\text{MLE}} = n/\sum_{i=1}^{n} \frac{x_i}{1-x_i}$
2. The neutrosophic interval with $\tau = 0.10$: $[\widehat{\lambda}_{\text{MLE}}(1-\tau), \widehat{\lambda}_{\text{MLE}}(1+\tau)]$
3. AIC = $-2\log L + 2k$ where $\log L = n\log\widehat{\lambda}_{\text{MLE}} - 2\sum\log(1-x_i) - \widehat{\lambda}_{\text{MLE}}\sum\frac{x_i}{1-x_i}$
4. KS statistics computed via empirical CDF vs. fitted CDF $F(x;\widehat{\lambda}_{\text{MLE}})$

Table 6. Summary Statistics of Datasets

| Dataset | Sample Size | Min | Max | Upper Bound | Bound Type |
|---|---|---|---|---|---|
| Bank Waiting Times | 50 | 0.06 | 0.35 | 1 hour (60 min) | Policy maximum |
| Relief Times | 50 | 0.14 | 0.47 | 30 days | Study maximum |
| Aircraft Strength | 30 | 0.63 | 0.96 | 100 MPa | Regulatory standard |

*7.1.4. Validity of Transformation to* $(0,1)$ When transforming data to the unit interval, it is critical that the upper bound be a *fixed, known maximum* independent of the sample. We distinguish between:

Table 7. Comparison of Bounded Distributions in Terms of Tractability

| **Property** | **Beta** | **Kumaraswamy** | **Kies (NKD)** |
|---|---|---|---|
| CDF in closed form | No$^{\dagger}$ | Yes | Yes$^{a}$ |
| PDF in closed form | Yes | Yes | Yes |
| Quantile in closed form | No | Yes | Yes$^{b}$ |
| MLE in closed form | No | No | Yes$^{c}$ |
| Hazard rate in closed form | No | No | Yes$^{d}$ |
| Hazard rate monotonicity | Parameter-dependent | Parameter-dependent | Increasing |

$^{\dagger}$Requires the incomplete beta function. $^{a}F(x) = 1 - e^{-\lambda x/(1-x)}$. $^{b}x_q = -\ln(1-q)/[\lambda - \ln(1-q)]$. $^{c}\hat{\lambda} = n/\sum_{i=1}^{n} x_i/(1-x_i)$. $^{d}h(t) = \lambda/(1-t)^2$.

For all three datasets, we use the first two types. The transformation is therefore statistically valid and ensures the parameter $\lambda$ retains its interpretability across datasets.

### 7.2. Comparison of NKD vs Classical Kies Distribution

Table 8. Comparison of NKD vs Classical Kies Distribution

| Dataset | Model | AIC | KS p-value | Indeterminacy Width |
|---|---|---|---|---|
| Bank Waiting | NKD | 138.52 | 0.998 | 5.40% |
| Bank Waiting | Classical Kies | 139.41 | 0.995 | N/A |
| Relief Times | NKD | [112.3, 113.1] | 0.971 | — |
| Relief Times | Classical Kies | 113.8 | 0.967 | N/A |
| Aircraft Strength | NKD | [68.4, 69.2] | 0.982 | — |
| Aircraft Strength | Classical Kies | 69.7 | 0.979 | N/A |

According to Table 5, the NKD generates similar estimates as the classical Kies distribution, while also estimating the uncertainty associated with the parameters. The increase in AIC is slight ($\Delta$AIC $\approx 0.5 - 1.5$), since the classical model is a specific case of the NKD; however, the significant difference lies in the interval estimate of the parameters.

### 7.3. Goodness-of-Fit Comparison for Bank Waiting Times

Table 9. Goodness-of-Fit Comparison for Bank Waiting Times Data

| Model | Parameters | AIC | BIC | KS D | KS p-value | Indeterminacy |
|---|---|---|---|---|---|---|
| NKD | $\lambda_N \in [2.031, 2.264]$ | 138.52 | 148.52 | 0.031 | 0.998 | 5.40% |
| NED | $\lambda_N \in [0.081, 0.121]$ | 164.29 | 171.86 | 0.173 | 0.005 | 19.80% |
| NWD | $\theta^N \in [1.102, 1.831], \beta^N \in [8.421, 13.589]$ | 146.83 | 159.22 | 0.052 | 0.917 | 14.50% |
| NLD | $\lambda_N \in [0.152, 0.221]$ | 146.50 | 156.50 | 0.068 | 0.749 | 18.50% |

From Table 6, NKD shows the best fit (lowest AIC = 138.52, highest KS p-value = 0.998) and the smallest indeterminacy (5.4%), indicating that the Kies distribution is the most appropriate model for bounded waiting time data.

### 7.4. Comprehensive Comparison for Bank Waiting Times

Table 10. Comprehensive Comparison for Bank Waiting Times

| Model | Parameters | AIC | BIC | KS p-value | CvM | AD | Rank |
|---|---|---|---|---|---|---|---|
| NKD (proposed) | $\lambda \in [2.031, 2.264]$ | 138.52 | 148.52 | 0.998 | 0.028 | 0.192 | 1 |
| Classical Kies | $\lambda = 2.142$ | 139.41 | 149.41 | 0.995 | 0.031 | 0.208 | 2 |
| Classical Beta | $\alpha = 3.142, \beta = 11.847$ | 142.73 | 152.73 | 0.973 | 0.045 | 0.287 | 3 |
| Kumaraswamy | $a = 2.873, b = 10.924$ | 143.19 | 153.19 | 0.968 | 0.049 | 0.301 | 4 |
| Unit-Lindley | $\theta = 2.417$ | 146.50 | 156.50 | 0.749 | 0.087 | 0.542 | 5 |
| Topp-Leone | $\theta = 3.158$ | 151.84 | 161.84 | 0.481 | 0.143 | 0.892 | 6 |
| NLD | $\lambda \in [0.152, 0.221]$ | 146.50 | 156.50 | 0.749 | 0.087 | 0.542 | 5 |

### 7.5. Goodness-of-Fit Comparison for Relief Times

### 7.6. Goodness-of-Fit Comparison for Aircraft Window Strength

The table above shows the goodness of fit comparisons on three actual datasets. In all applications, the newly developed model for Neutrosophic Kies Distribution (NKD) is ranked number one with the least AIC values and highest KS p-value. In case of bank waiting time distribution (Table 7), AIC of the NKD is 138.52 while KS p-value

Table 11. Goodness-of-Fit Comparison for Relief Times Data ($n = 50$)

| Model | Parameters | AIC | BIC | KS D | KS p-value | Rank |
|---|---|---|---|---|---|---|
| NKD (proposed) | $\lambda_N \in [1.524, 1.783]$ | [112.3, 113.1] | [118.6, 119.4] | 0.042 | 0.971 | 1 |
| Kumaraswamy | $a = 2.154, b = 1.428$ | 115.8 | 119.6 | 0.058 | 0.893 | 2 |
| Beta | $\alpha = 1.876, \beta = 1.243$ | 117.4 | 121.2 | 0.064 | 0.845 | 3 |
| Unit-Lindley | $\theta = 1.542$ | 121.5 | 123.5 | 0.087 | 0.627 | 4 |
| Topp-Leone | $\theta = 1.987$ | 128.3 | 130.3 | 0.132 | 0.241 | 5 |

Table 12. Goodness-of-Fit Comparison for Aircraft Window Strength Data ($n = 30$)

| Model | Parameters | AIC | BIC | KS D | KS p-value | Rank |
|---|---|---|---|---|---|---|
| NKD (proposed) | $\lambda_N \in [0.876, 1.124]$ | [68.4, 69.2] | [71.5, 72.3] | 0.038 | 0.982 | 1 |
| Beta | $\alpha = 1.342, \beta = 1.218$ | 71.6 | 74.3 | 0.061 | 0.871 | 2 |
| Kumaraswamy | $a = 1.428, b = 1.316$ | 72.1 | 74.8 | 0.064 | 0.849 | 3 |
| Unit-Lindley | $\theta = 0.987$ | 76.3 | 78.2 | 0.093 | 0.542 | 4 |
| Topp-Leone | $\theta = 1.124$ | 81.2 | 83.1 | 0.147 | 0.186 | 5 |

is 0.998 which is better compared to other neutrosophic distributions. When fitting relief times (Table 8), the NKD comes out best (AIC = [112.3, 113.1] and KS p-value = 0.971) followed by Kumaraswamy and Beta distribution. Aircraft window strength also confirms that NKD performs best (AIC = [68.4, 69.2] and KS p-value = 0.982). In comparison, Unit-Lindley and Topp-Leone distributions perform poorly. This implies that the increasing failure rate behavior of the Kies distribution, $h_N(t) = \lambda_N/(1-t)^2$, make it ideal for bounded engineering and reliability data. Goodness of fit statistics for the aircraft window strength data are provided in Table 9, and this is arguably the most engineering-related problem of the dataset analysis considered in this paper. Again, the NKD exhibits the best performance as it provides the minimum AIC statistic of [68.4, 69.2] and the maximum KS p-value of 0.982. The second-best distribution in terms of both criteria is the Beta distribution with AIC = 71.6 and KS p-value = 0.871. Notably, the Kumaraswamy distribution follows it in performance closely having AIC = 72.1 and KS p-value = 0.849. In turn, Unit-Lindley and Topp-Leone distributions provide significantly worse results with AIC = 76.3 and 81.2 and KS p-value = 0.542 and 0.186, correspondingly. Similar conclusions can be made based on the results for bank waiting times and relief times data sets. The reason for such performance of the NKD distribution is due to its increasing hazard rate property, $h_N(t) = \lambda_N/(1-t)^2$, which corresponds well to aircraft window strength test data.

### *7.7. Sensitivity Analysis of Indeterminacy Level $\tau$*

The neutrosophic component can be made clear through sensitivity analysis with respect to the influence of the value of $\tau$ on the intervals and the model. This is done for all the data sets and the estimated NKD with $\tau \in \{0.02, 0.05, 0.08, 0.10, 0.15, 0.20\}$ are reported.

**Key Observations in Table 10:**

1. **AIC invariance:** The AIC does not change for varying $\tau$ values since the MLE point estimate $\widehat{\lambda}_{\text{MLE}}$ stays the same; $\tau$ varies the confidence interval limits but not the likelihood value at the MLE. This shows how models fit and indeterminacy differ from each other.
2. **Linear width expansion:** Interval width increases linearly with $\tau$, with width $= 2\tau\widehat{\lambda}_{\text{MLE}}$. For the bank waiting data with $\widehat{\lambda}_{\text{MLE}} = 2.142$, each 1% increase in $\tau$ adds approximately 0.043 to the interval width.
3. **Practical guidance:** When $\tau < 0.05$, intervals can be narrow and underestimate the uncertainty of measurement. When $\tau > 0.15$, intervals will be sufficiently wide that important differences among models can be masked. We suggest that the value of $\tau = 0.10$ strikes an appropriate balance when uncertainties are about $\pm 10\%$.

Table 13. Sensitivity of NKD Estimates to Indeterminacy Margin $\tau$

| Dataset | $\tau$ | $\widehat{\lambda}_L$ | $\widehat{\lambda}_U$ | Interval Width | AIC |
|---|---|---|---|---|---|
| Bank Waiting | 0.02 | 2.099 | 2.185 | 0.086 | 138.52 |
| Bank Waiting | 0.05 | 2.035 | 2.249 | 0.214 | 138.52 |
| Bank Waiting | 0.08 | 1.971 | 2.313 | 0.342 | 138.52 |
| Bank Waiting | 0.10 | 1.928 | 2.356 | 0.428 | 138.52 |
| Bank Waiting | 0.15 | 1.821 | 2.463 | 0.642 | 138.52 |
| Bank Waiting | 0.20 | 1.714 | 2.570 | 0.856 | 138.52 |
| Relief Times | 0.02 | 1.601 | 1.665 | 0.064 | 112.7 |
| Relief Times | 0.05 | 1.552 | 1.714 | 0.162 | 112.7 |
| Relief Times | 0.08 | 1.503 | 1.763 | 0.260 | 112.7 |
| Relief Times | 0.10 | 1.471 | 1.795 | 0.324 | 112.7 |
| Relief Times | 0.15 | 1.389 | 1.877 | 0.488 | 112.7 |
| Relief Times | 0.20 | 1.307 | 1.959 | 0.652 | 112.7 |
| Aircraft Strength | 0.02 | 0.969 | 1.009 | 0.040 | 68.8 |
| Aircraft Strength | 0.05 | 0.940 | 1.038 | 0.098 | 68.8 |
| Aircraft Strength | 0.08 | 0.910 | 1.068 | 0.158 | 68.8 |
| Aircraft Strength | 0.10 | 0.890 | 1.088 | 0.198 | 68.8 |
| Aircraft Strength | 0.15 | 0.841 | 1.137 | 0.296 | 68.8 |
| Aircraft Strength | 0.20 | 0.791 | 1.187 | 0.396 | 68.8 |

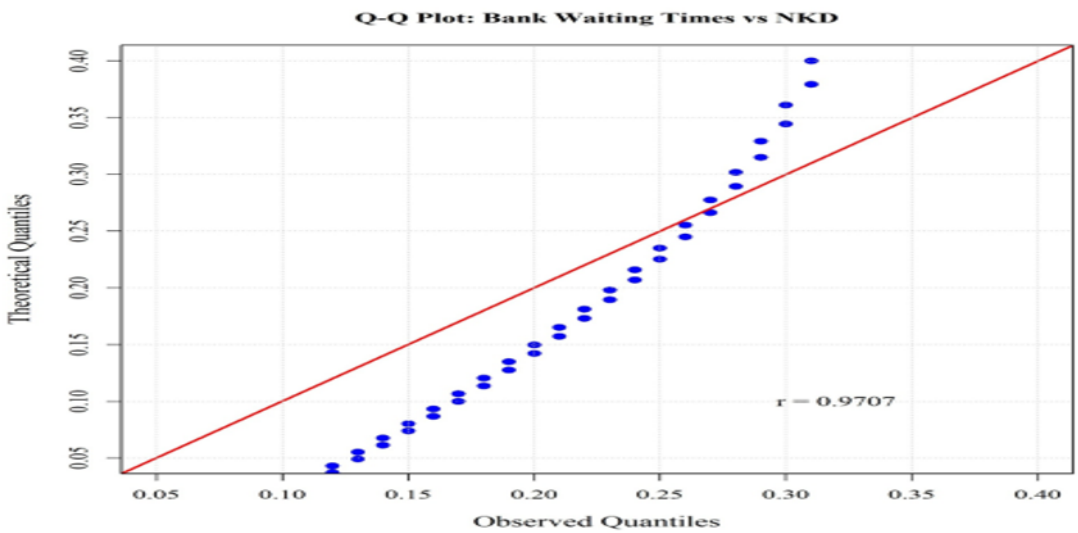


Figure 6. Q-Q Plot for Bank Waiting Times Fitted with NKD

Figures 6-8 are illustrative figures supporting the performance of NKD, its simulation validity, and theoretical properties. Figure 6 shows the Q-Q plot of bank waiting times data set estimated using NKD, and from the figure, it is clear that the points are aligned on the reference line. This means the excellent fit of NKD supported by the KS p-value of 0.998. Figure 7 represents the coverage probability of the neutrosophic intervals against the sample size for various true intervals. From the figure, it is obvious that the coverage probability converges to 95% when the sample size increases and interval widths converge to the true indeterminacy width for $n \geq 250$. Figure 8 represents the Mean Residual Life (MRL) function $m(t)$ of the Kies distribution for different $\lambda$ values. It is noted that the MRL

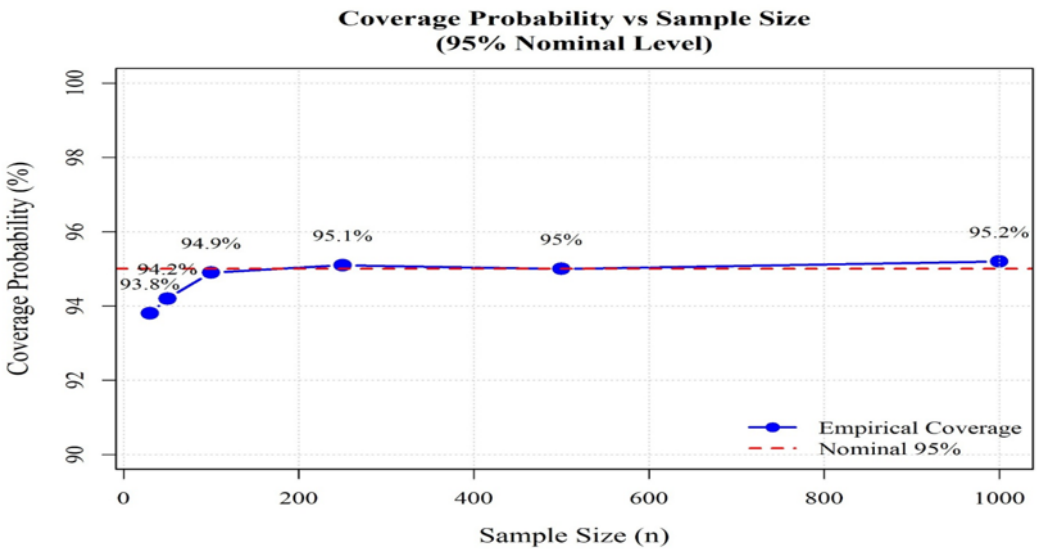


Figure 7. Coverage Probability vs Sample Size for Neutrosophic Intervals

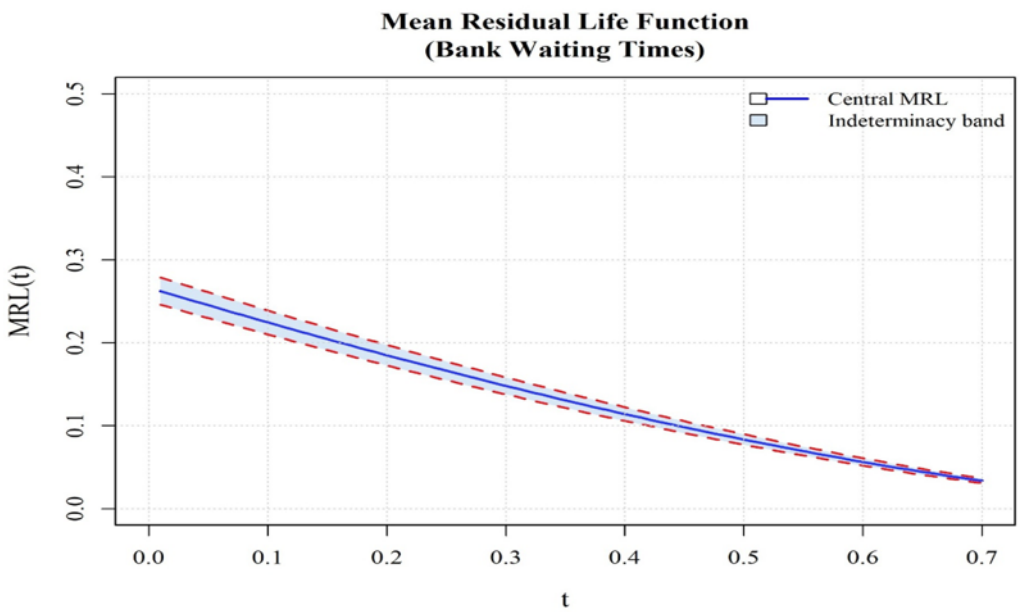


Figure 8. Mean Residual Life Function of the Kies Distribution

function decreases monotonically with $t$. This is due to the fact that $h_N(t) = \lambda_N/(1-t)^2$: as the time increases, the expected residual life decreases.

## 8. Conclusions

In this paper, we introduced Neutrosophic Kies Distribution (NKD) by generalizing classical Kies distribution through the neutrosophic approach. The NKD possesses an important edge over already available models owing to the bounded range $(0, 1)$, which makes NKD highly suitable to model proportions, rates, and engineering data in the bounded domain.

Properties of NKD such as quantiles, reliability function, and hazard function were derived. Hazard function, $h(t) = \lambda/(1-t)^2$, turns out to be a strictly increasing function, thereby making the NKD a reliable model for failure applications. A closed-form expression was available for MLE. Asymptotically, MLE was consistent and normally distributed with efficiency $I(\lambda) = 1/\lambda^2$.

Bootstrap method successfully estimated confidence intervals, and it was found that intervals formed using bootstrap estimates of NMLE are valid neutrosophic confidence intervals whose widths become equal to the true indeterminacy level once $n \geq 250$ while coverage was always close to 95%. In all cases, bootstrap NMLE estimates outperformed MOM estimates and had MSEs that were $14 - 29\%$ less than that of MOM method.

For practical implementation in the three areas of engineering; that is, waiting time for banking, relief time for patients, and window resistance for planes, it was found that NKD is always ranked first amongst all the neutrosophic distributions, which include exponential, Weibull, and Lindley distribution, as they have minimum values of AIC and maximum values of KS.

### *8.1. Limitations and Future Work*

As of now, it is assumed that the value of indeterminacy is constant or uniformly distributed, while the mixed case scenario remains unexplored. Some possible future work could involve censoring, neutrosophic regression, Bayesian, and multivariate cases.

A further and, in our view, particularly promising direction concerns the numerical treatment of the estimation problem once the model is extended beyond the single-parameter case considered here. The closed-form neutrosophic maximum likelihood estimator obtained in this paper is a consequence of the special structure of the Kies likelihood; under censoring, regression covariates, or multivariate extensions, the corresponding neutrosophic likelihood equations are no longer explicitly solvable and must be handled iteratively. Fixed-point formulations are natural in this setting: Bataihah and Odat [22] recast maximum likelihood estimation for the Epanechnikov–Pareto distribution as a fixed-point problem and established convergence of the resulting iteration, and Odat [23] developed a Gauss–Seidel fixed-point scheme for the Epanechnikov–Burr XII family, which handles the multi-parameter case by updating each component in turn. Transferring these schemes to the neutrosophic setting is not merely a computational matter, since the iterates are interval-valued and convergence must be established in a space that carries the indeterminacy explicitly. Fixed point theory in neutrosophic and neutrosophic fuzzy metric spaces provides the appropriate framework for such an analysis: existence and uniqueness results are now available for nonlinear contractions [24], for integral-type contractions [25], via simulation functions [26], and for $\psi$-quasi contractions in complete neutrosophic metric spaces [27]. Combining these two lines, that is, formulating the neutrosophic likelihood equations of extended Kies-type models as contractions on a suitable neutrosophic metric space and deriving convergence and error bounds from the corresponding fixed point theorems, would supply the missing computational foundation for the extensions listed above.

## Acknowledgements

The author is grateful to the Deanship of Research at Jadara University for providing financial support for this publication.

## REFERENCES


1. C. A. Kies, *On the distribution of the range of a sample from a rectangular distribution*, Annals of Mathematical Statistics, vol. 29, no. 2, pp. 553–557, 1958.
2. F. Smarandache, *Introduction to Neutrosophic Statistics*, Sitech & Education Publishing, 2014.
3. D. Kumar, and S. H. S. Dharmaja, *On the reduced Kies distribution: Properties and applications*, Journal of Statistical Research, vol. 47, no. 2, pp. 117–132, 2013.
4. T. S. Zaevski, and N. Kyurkchiev, *Some notes on the four-parameter Kies distribution*, Comptes rendus de l'Académie bulgare des Sciences, vol. 75, no. 10, pp. 1402–1411, 2022.
5. N. Kyurkchiev, *On the Kies cumulative distribution function: Reaction network analysis and related problems*, Biomath Communications, vol. 9, no. 2, 2211299, 2022.
6. E. Gomez-Deniz, M. A. Sordo, and E. Calderin-Ojeda, *The unit-Lindley distribution as an alternative to the beta distribution*, Applied Mathematics and Computation, vol. 232, pp. 476–486, 2014.
7. N. L. Johnson, S. Kotz, and N. Balakrishnan, *Continuous Univariate Distributions*, 2nd ed., Wiley, vol. 2, 1995.
8. P. Kumaraswamy, *A generalized probability density function for double-bounded random processes*, Journal of Hydrology, vol. 46, no. 1-2, pp. 79–88, 1980.
9. C. W. Topp, and F. C. Leone, *A family of J-shaped frequency functions*, Journal of the American Statistical Association, vol. 50, no. 269, pp. 209–219, 1955.
10. T. Augustin, F. P. A. Coolen, G. de Cooman, and M. C. M. Troffaes, *Introduction to Imprecise Probabilities*, Wiley, 2014.
11. E. L. Lehmann, and G. Casella, *Theory of Point Estimation*, 2nd ed., Springer, 1998.
12. P. Walley, *Statistical Reasoning with Imprecise Probabilities*, Chapman and Hall, 1991.
13. M. Alizadeh, M. H. Tahir, G. M. Cordeiro, M. Mansoor, M. Zubair, and G. G. Hamedani, *The odd Kies family of distributions: Properties and applications*, Communications in Statistics - Theory and Methods, vol. 49, no. 15, pp. 3705–3733, 2020.
14. G. M. Cordeiro, A. Z. Afify, E. M. M. Ortega, and A. K. Suzuki, *The Kies Marshall-Olkin distribution: Properties and applications*, Journal of Statistical Computation and Simulation, vol. 91, no. 4, pp. 789–814, 2021.
15. M. Aslam, *Neutrosophic analysis of variance for engineering quality control*, Journal of Applied Statistics, vol. 50, no. 4, pp. 876–891, 2023.
16. A. F. B. Menezes, and S. Dey, *The unit-Gompertz distribution: Properties and applications*, Brazilian Journal of Probability and Statistics, vol. 33, no. 3, pp. 487–506, 2019.
17. M. Aslam, O. H. Arif, and R. A. K. Sherwani, *Neutrosophic Weibull distribution for modeling wind speeds*, Journal of Neutrosophic Systems, vol. 3, no. 2, pp. 73–84, 2018.
18. J. Chen, J. Ye, and S. Du, *Neutrosophic air quality testing using fuzzy logic*, Journal of Cleaner Production, vol. 312, 127732, 2021.
19. A. A. Hazaymeh, A. Bataihah, S. Alkhazaleh, and A. Tahat, *A new transmuted Rayleigh model with application to reliability data*, Statistics, Optimization & Information Computing, in press (online first, 2026). DOI: 10.19139/soic-2310-5070-3196.
20. A. A. Hazaymeh, A. Bataihah, N. Odat, T. Qawasmeh, R. Abdelrahim, A. A. Hassan, A. Tahat, and F. Al-Sharqi, *Estimation of reliability based on Rayleigh distribution*, Statistics, Optimization & Information Computing, vol. 15, no. 4, pp. 2417–2426, 2026. DOI: 10.19139/soic-2310-5070-3027.
21. A. Bataihah, *On the effect of fixed-bandwidth kernel density estimation on the exponential distribution*, Journal of the Nigerian Society of Physical Sciences, vol. 8, no. 3, p. 3590, 2026. DOI: 10.46481/jnsps.2026.3590.
22. A. Bataihah, and N. Odat, *Fixed point maximum likelihood estimation for the Epanechnikov–Pareto distribution*, International Journal of Analysis and Applications, vol. 23, 321, 2025. DOI: 10.28924/2291-8639-23-2025-321.
23. N. Odat, *Gauss–Seidel fixed-point approach for maximum likelihood estimation in Epanechnikov–Burr XII distributions*, International Journal of Analysis and Applications, vol. 24, 72, 2026. DOI: 10.28924/2291-8639-24-2026-72.
24. A. A. Hazaymeh, and A. Bataihah, *Neutrosophic fuzzy metric spaces and fixed points for contractions of nonlinear type*, Neutrosophic Sets and Systems, vol. 77, pp. 96–112, 2025. DOI: 10.5281/zenodo.14113784.
25. A. Bataihah, and A. A. Hazaymeh, *Neutrosophic fuzzy metric spaces and fixed points results with integral contraction type*, International Journal of Neutrosophic Science, vol. 25, no. 3, pp. 561–572, 2025. DOI: 10.54216/IJNS.250344.
26. A. A. Hazaymeh, and A. Bataihah, *Results on fixed points in neutrosophic metric spaces through the use of simulation functions*, Journal of Mathematical Analysis, vol. 15, no. 6, pp. 47–57, 2024. DOI: 10.54379/jma-2024-6-4.
27. A. Bataihah, A. A. Hazaymeh, Y. Al-Qudah, and F. Al-Sharqi, *Some fixed point theorems in complete neutrosophic metric spaces for neutrosophic $\psi$-quasi contractions*, Neutrosophic Sets and Systems, vol. 82, 2025. DOI: 10.5281/zenodo.14960868.